SUPPORTING INFORMATION

Nitrate Sensing with Molecular Cage Ionophores: A Potentiometric Approach

Ahmet Onder, Ferit Begar, Erman Kibris, Onur Buyukcakir,* and Umit Hakan Yildiz*

Department of Chemistry, Izmir Institute of Technology, Izmir 35430, Turkey.

E-mail: onurbuyukcakir@iyte.edu.tr, hakanyildiz@iyte.edu.tr

1. Materials and Methods

1.1 Materials

Starting materials, reagents, and solvents were purchased from Sigma Aldrich Chemical Co. (4'-hydroxyacetophenone, cyanuric chloride, N,N-dimethylamine solution 40 wt. % in H_2O, $CDCl_3$), Tokyo Chemical Industry Co.-TCI (silicon tetrachloride, N,N-Diisopropylethylamine, phloroglucinol) and Carlo Erba Reagents (acetonitrile, acetone, THF, DMF, toluene, methanol, ethanol). They were utilized as received with no additional purification unless otherwise specified. 1,3,5-Tris(4-hydroxyphenyl)benzene[S1], CAGE-0[S2], and CAGE-1[S3] were synthesized following the reported procedures with modifications. The synthesized compounds were purified through column chromatography using Merck Kieselgel 60 H silica gel (70 – 230 mesh) as a solid phase. All chemicals and sodium and potassium salts of the anions used were supplied from Sigma-Aldrich. Deionized water was used in all experimental studies.

1.2 Methods

1.2.1 Material Characterization Methods

^1H and ^{13}C spectra were acquired with Varian 400 MHz NMR Spectrometer (^1H NMR: 400 MHz; ^{13}C NMR: 100 MHz) at ambient temperature. Chemical shifts reported in parts per million (ppm) relative to the residual non-deuterated solvent signals ($CDCl_3$: δ 7.26 ppm, DMSO-*d6*: δ 2.50 ppm) Fourier transform infrared (FT-IR) measurements were recorded using Perkin-Elmer 100 FT-IR spectrometers, and samples were analyzed as KBr disks in the transmission mode under ambient temperature and humidity. The mass spectra were recorded using Agilent 6530 Q-TOF LC/MS.

2. Synthesis

2.1 Synthesis of CLEFT-0

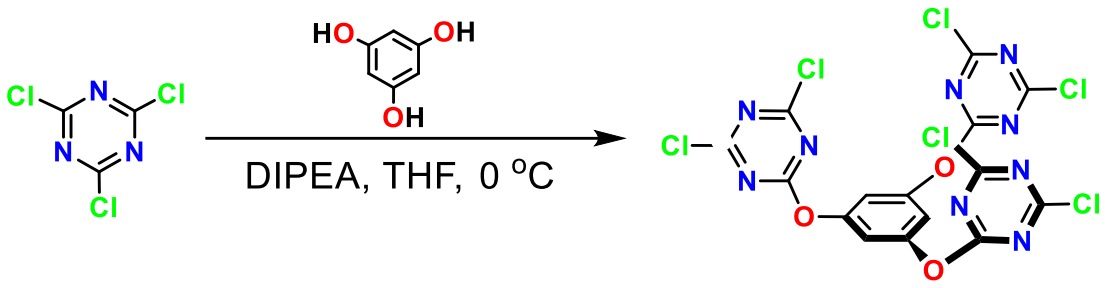

To an ice-cooled solution of cyanuric chloride (2.5 g, 13.5 mmol) in THF (50 mL) was added a mixture of phloroglucinol (0.38 g, 3.0 mmol) and DIPEA (1.5 g, 2.0 mL, 11.3 mmol) in THF (20 mL) over a period of one hour at 0 °C. The resulting suspension was further stirred for 4 hours at 0 °C. After the completion of the reaction, the precipitate was filtered, and the filtrate was concentrated under a vacuum. The crude product was washed with a mixture of DCM / Hexane (1 : 5) three times (20 ml) to afford the pure product, CLEFT-0, as a white solid (1.2 g, 70%). ^{1}H NMR ($CDCl_3$, 400 MHz, 25 °C) δ (ppm) = 7.17 (s, 3 H); ^{13}C NMR ($CDCl_3$, 100 MHz, 25 °C) δ (ppm) = 173.5, 170.4, 151.7, 113.8.

2.2 Synthesis of CAGE-0

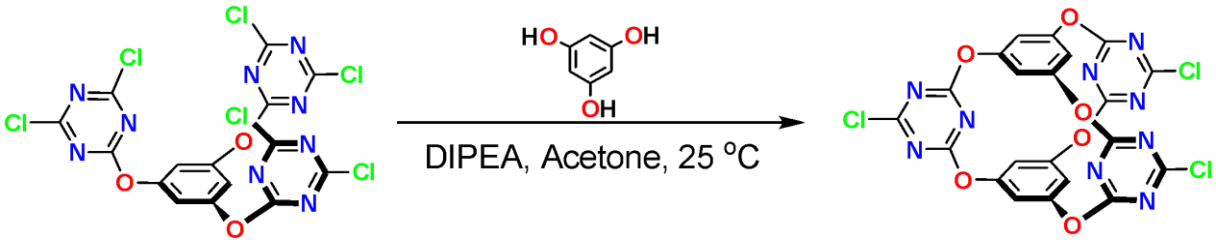

To a solution of DIPEA (2.0 g, 2.6 mL, 15.2 mmol) in acetone (150 mL) was added CLEFT-0 (2.4 g, 4.2 mmol) in acetone (100 ml) and phloroglucinol (0.53 g, 4.2 mmol) in acetone (100 mL) at the same rate over 6 hours at room temperature. The resulting mixture was stirred further at room temperature for three days. After the completion of the reaction, the solvent was removed under reduced pressure, and the crude product was purified by column chromatography on silica gel [DCM / EtOAc (100 : 2)] to yield the pure product, CAGE-0, as a white solid (0.76 g, 31%). ^{1}H NMR ($CDCl_3$, 400 MHz, 25 °C) δ (ppm) = 6.69 (s, 6 H); ^{13}C NMR ($CDCl_3$, 100 MHz, 25 °C) δ (ppm) = 175.1, 172.7, 153.1 115.05. QTOF-HRMS calcd for m/z = 585.9585 $[M+H]^+$, found m/z = 585.9601 $[M+H]^+$.

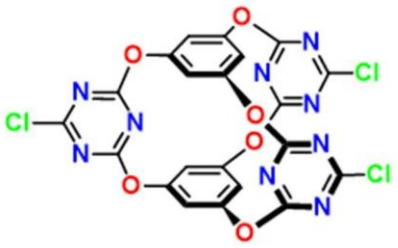

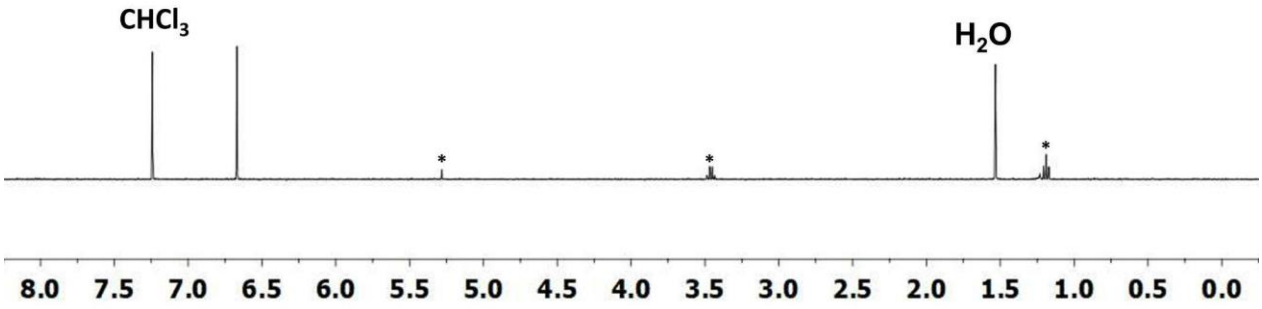

2.3 Synthesis of CAGE-2

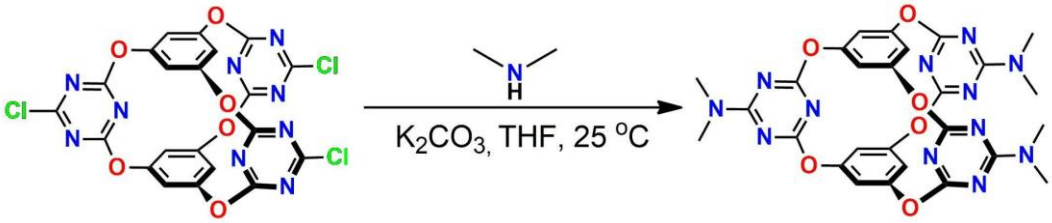

To a solution of CAGE-0 (50 mg, 0.085 mmol) and K_2CO_3 (42 mg, 0.31 mmol) in THF (10 mL) was added N.N'-dimethylamine solution (65 µL from %40 solution). The resulting mixture was stirred at room temperature for 2 hours. After the completion of the reaction, the solvent was removed under reduced pressure. The crude product was extracted with DCM (3 x 15 mL), and combined organic phases were dried over $MgSO_4$. The solvent was removed under reduced pressure to afford the pure product, CAGE-2, as a white solid (52 mg, 85%). ^{1}H NMR (400 MHz, $CDCl_3$, 25 °C) δ (ppm) = 6.52 (s, 6H), 3.24 (s, 18H); ^{13}C NMR ($CDCl_3$, 100 MHz, 25 °C) δ (ppm) = 172.2, 167.9, 153.0, 115.1, 36.9. QTOF-HRMS calcd for m/z = 613.2020 $[M+H]^+$, found m/z = 613.2024 $[M+H]^+$.

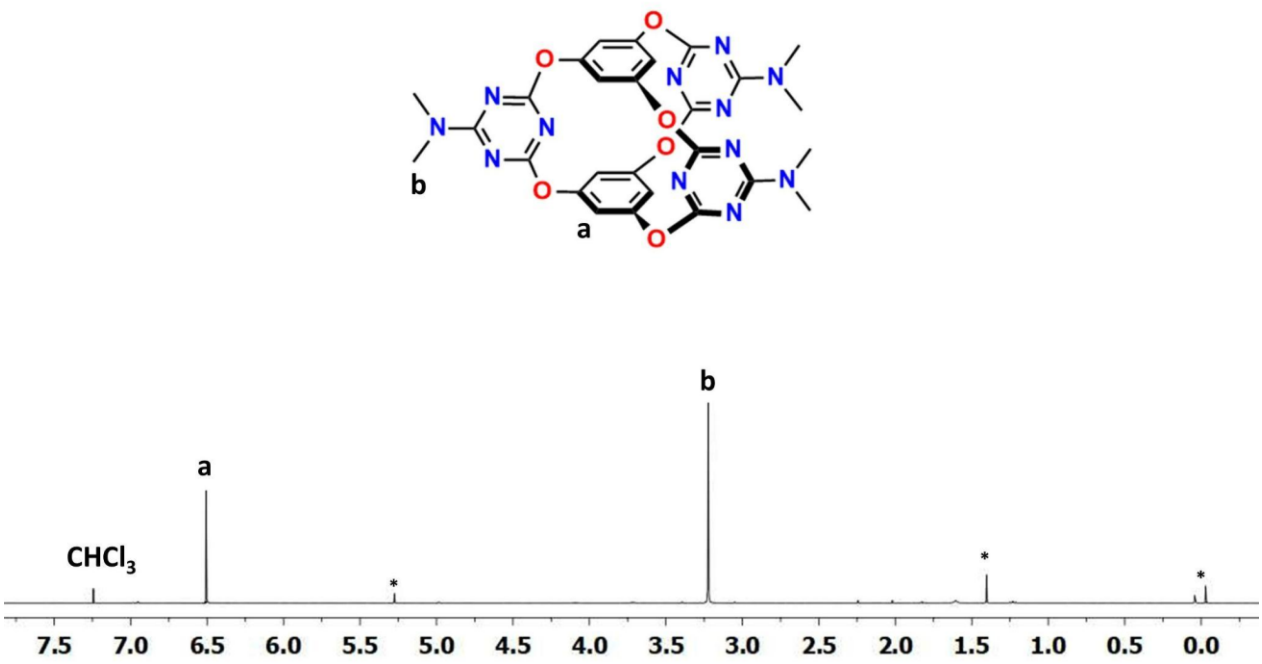

2.4 Synthesis of 1,3,5-Tris(4-hydroxyphenyl)benzene

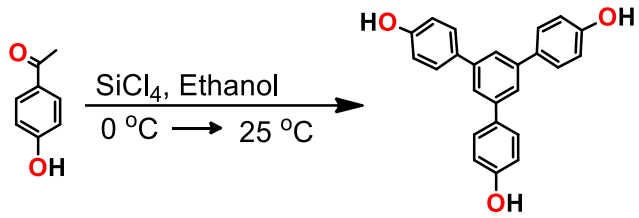

To an ice-cooled solution of 4-hydroxyacetophenone (2.0 g, 14.7 mmol) in ethanol (50 mL) was added silicon tetrachloride (17.6 g, 11.8 mL, 102.9 mmol) dropwise. The reaction mixture was gradually heated to 25 °C and stirred for 24 hours at room temperature. After the completion of the reaction, the mixture was quenched by adding water and extracted with ethyl acetate (3 x 100 mL). The organic phases are combined and dried over $MgSO_4$. The solvent was removed under reduced pressure, and the crude product was purified by column chromatography on silica gel [DCM / EtOAc (100 : 8)] to yield pure product, 1,3,5-Tris(4-hydroxyphenyl)benzene, as purple solid (3.90 g, 75%). ^{1}H NMR (Acetone-d_6, 400 MHz, 25 °C) δ (ppm) = 8.91 (s, 3H), 8.14 (s, 3H), 8.11 (d, J = 8.5 Hz, 6H), 7.42 (d, J = 8.5 Hz, 6H); ^{13}C NMR (100 MHz, Acetone-d_6, 25 °C): δ (ppm) = 158.1, 142.9, 133.4, 129.2, 123.6, 116.5.

2.5 Synthesis of CLEFT-1

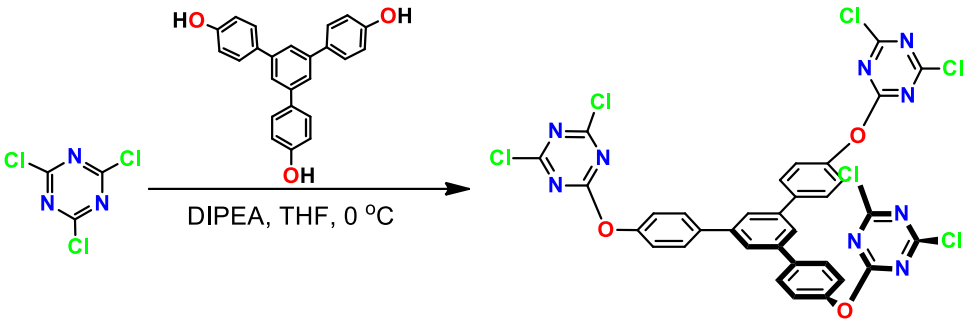

A mixture of 1,3,5-Tris(4-hydroxyphenyl)benzene (3.5 g, 10 mmol) and DIPEA (5.0 g, 7.8 mL, 39 mmol) was added to a solution of cyanuric chloride (8.3 g, 45 mmol) at 0 °C over 1.5 hours. The resulting suspension was further stirred for 6 hours at 0 °C. After the completion of the reaction, the precipitate was filtered, and the filtrate was concentrated under a vacuum. The crude product was washed with a mixture of DCM / Hexane (1 : 10) three times (20 ml) to afford the pure product, CLEFT-1, as a white solid (5.7 g, 72%). ^{1}H NMR ($CDCl_3$, 400 MHz, 25 °C) δ (ppm) = 7.83 (s, 3H), 7.80 (d, J = 8.6 Hz, 6H), 7.34 (d, J = 8.6 Hz, 6H); ^{13}C NMR (100 MHz, $CDCl_3$, 25 °C): δ (ppm) = 173.2, 171.1, 150.8, 141.4, 139.6, 128.8, 125.4, 121.5.

2.6 Synthesis of CAGE-1

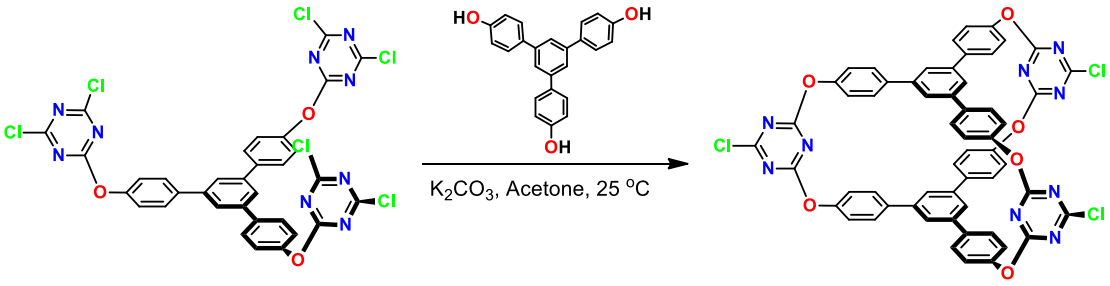

To a suspension of well-grinded K_2CO_3 (620.0 mg, 4.5 mmol) in acetone (250 mL), CLEFT-1 (1.0 g, 1.3 mmol) solution in acetone (150 mL) and 1,3,5-Tris(4-hydroxyphenyl)benzene (445.0 mg, 1.3 mmol) in acetone (150 mL) were added at the same rate and time over 6 hours at room temperature. The resulting mixture was further stirred at room temperature for three days. After the completion of the reaction, the solution was filtered, and the filtrate was concentrated under reduced pressure. The crude product was purified by column chromatography on silica gel [DCM / EtOAc (100 : 2)] to yield the pure product, CAGE-1, as a white solid (271.2 mg, 25%). ^{1}H NMR (DMSO-*d6*, 400 MHz, 25 °C) δ (ppm) = 7.86 (d, J = 8.5 Hz, 12H), 7.68 (s, 6H), 7.31 (d, J = 8.5 Hz, 12H);

^{13}C NMR (100 MHz, DMSO-*d6*, 25 °C): δ (ppm) = 172.5, 171.7, 150.7, 139.6, 137.2, 127.6, 122.9, 121.5. QTOF-HRMS calcd for m/z = 1042.1463 $[M+H]^+$, found m/z = 1042.1478 $[M+H]^+$.

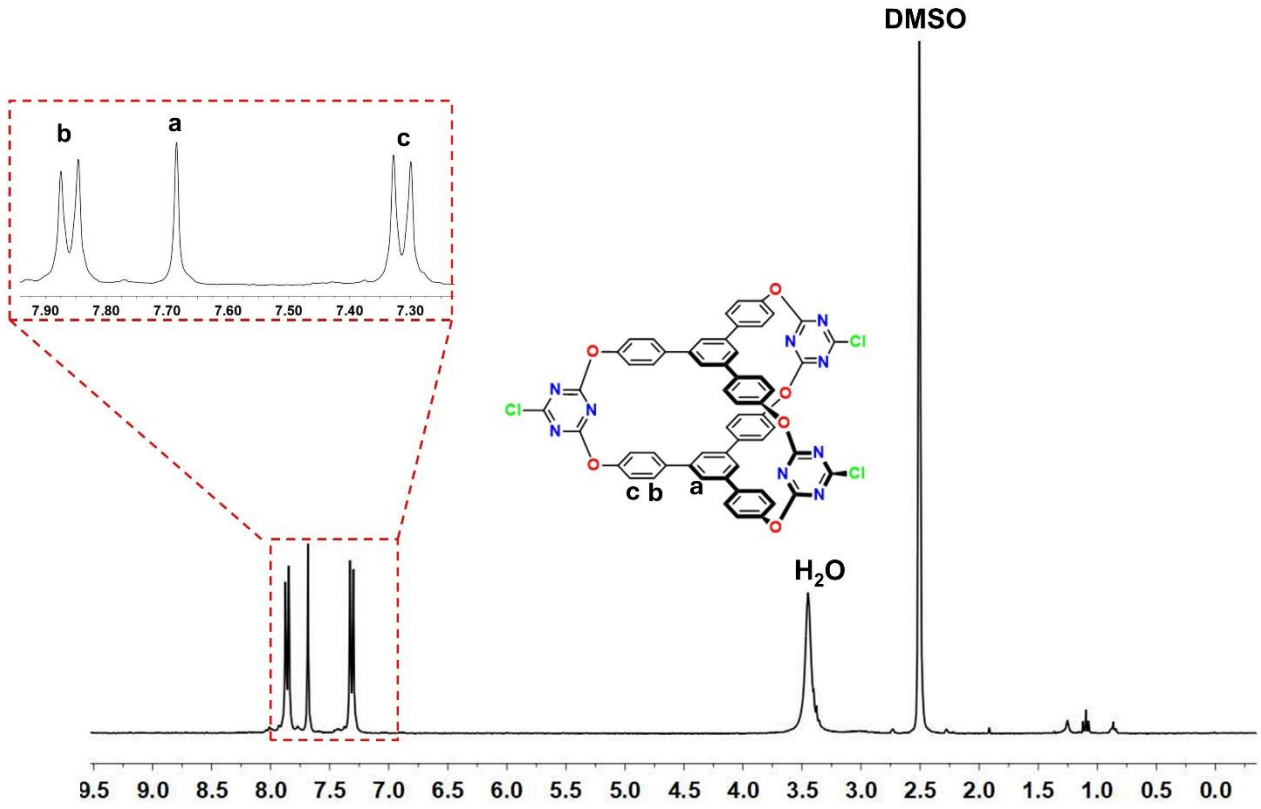

2.7 Synthesis of CAGE-3

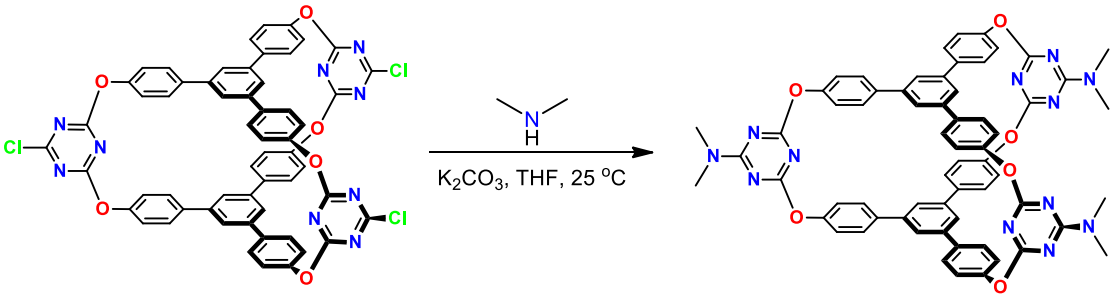

To a solution of CAGE-1 (30 mg, 0.029 mmol) and K_2CO_3 (23.8 mg, 0.17 mmol) in THF (5 mL) was added N.N'-dimethylamine solution (22 µL from %40 solution). The resulting mixture was stirred at room temperature for 2 hours. After the completion of the reaction, the solvent was removed under reduced pressure. The crude

product was extracted with DCM (3 x 15 mL), and combined organic phases were dried over $MgSO_4$. The solvent was removed under reduced pressure to afford the pure product, CAGE-3, as a white solid (29.4 mg, 95%).^{1}H NMR ($CDCl_3$, 400 MHz, 25 ^{o}C) δ (ppm) = 7.42 (d, J = 8.5 Hz, 12H), 7.31(s, 6H), 6.90 (d, J = 8.5 Hz, 12H), 3.28 (s, 18H); ^{13}C NMR (100 MHz, $CDCl_3$, 25 ^{o}C): δ (ppm) = 171.9, 168.4, 151.8, 141.0, 137.9, 126.9, 123.6, 122.7, 37.0. QTOF-HRMS calcd for m/z = 1069.3898 $[M+H]^+$, found m/z = 1069.3933 $[M+H]^+$.

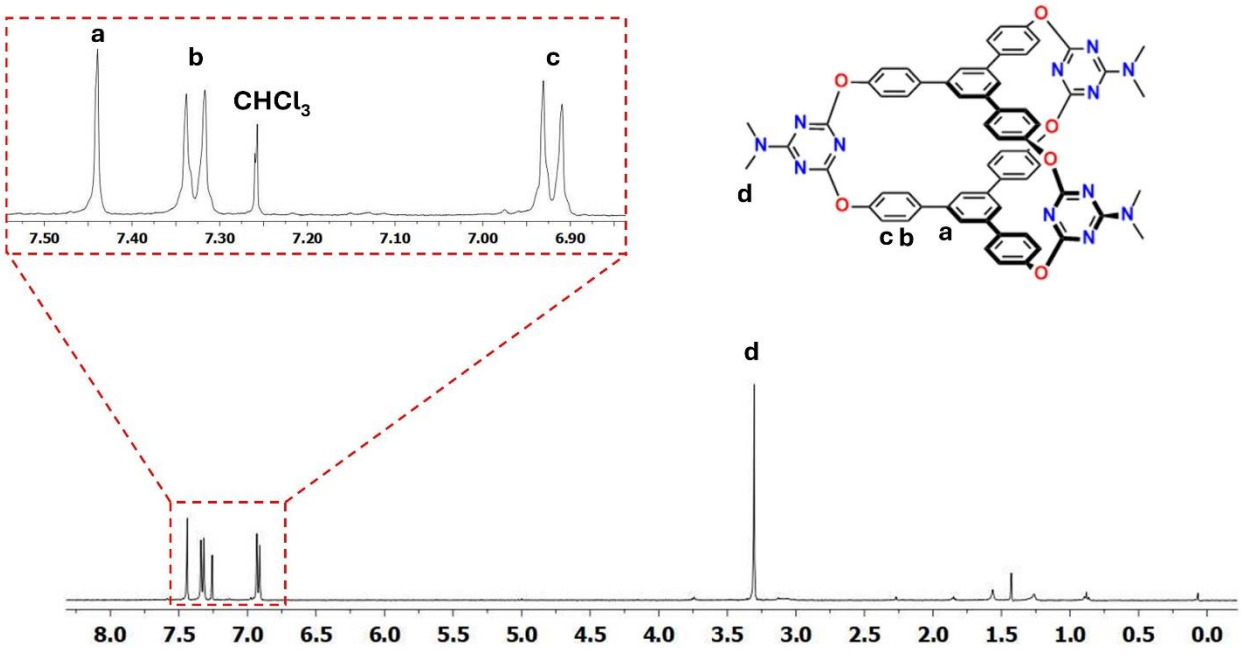

3. Comparison of ionophores of nitrate selective electrodes

Table S1: Ionophore comparison for nitrate selective electrodes

Ionophore	**Slope, mV dec^{-1}**	**LRR (M)**	**LOD (M)**	**Ref.**
TDMAN	-55.4	2.9×10^{-4}–1.7×10^{-1}	2.04×10^{-4}	[S4]
TDMAN	-58.2	5.0×10^{-4}–1.0×10^{-1}	6.01×10^{-6}	[S5]
TDMAN	-56.8	1.0×10^{-7}–1.0×10^{-2}	1.04×10^{-8}	[S6]
TDMAN	-56.8	1.0×10^{-6}–1.0×10^{-1}	3.16×10^{-7}	[S7]
TDMAN	-57.8	1.0×10^{-6}–1.0×10^{-1}	1.12×10^{-6}	[S7]
TDMAN	-54.8	5.0×10^{-5}–1.0×10^{-1}	2.5×10^{-6}	[S8]
TDMAN	-64.0	7.1×10^{-4}–1.0×10^{-1}	9.2×10^{-5}	[S9]
PPy-NO_3	-50.9	1.0×10^{-5}–5.0×10^{-1}	4.64×10^{-6}	[S10]
PPy-NO_3	-50.4	5.3×10^{-5}–1.0×10^{-1}	5.25×10^{-5}	[S11]
Nitrate ionophore VI	-54.1	5.0×10^{-5}–1.0×10^{-1}	-	[S12]
Nitrate ionophore VI	-60.0	4.0×10^{-5}–1.0×10^{-1}	4.0×10^{-6}	[S13]
$Co(Bphen)_2(NO_3)_2(H_2O)_2$	-57.1	1.0×10^{-6}–1.0×10^{-1}	5.0×10^{-7}	[S14]
$Co(Bphen)_2(NO_3)_2(H_2O)_2$	-56.3	1.0×10^{-5}–1.0×10^{-1}	3.98×10^{-6}	[S15]
$TDANO_3$	-59.1	1.0×10^{-6}–1.0×10^{-1}	7.59×10^{-7}	[S16]
$TDANO_3$	-53.7	1.0×10^{-5}–1.0×10^{-1}	1.3×10^{-6}	[S17]
Nit^+/NO_3	-55.1	8.0×10^{-8}–1.0×10^{-2}	2.8×10^{-8}	[S18]
$THANO_3$	-53.3	1.0×10^{-5}–1.0×10^{-1}	1.0×10^{-6}	[S19]
Nitrate ionophore V	-58.5	1.0×10^{-5}–1.0×10^{-1}	1.6×10^{-6}	[S20]
CAGE-1	**-53.1**	**1.0×10^{-5}–1.0×10^{-1}**	**7.5×10^{-6}**	**Our work**

Notes: LRR: Linear response range, **LOD:** Limit of Detection, **TDMAN**: Tridodecylmethylammonium nitrate, **POT-MoS_2**: Poly(3-octylthiophene)-Molybdenum Disulfide, **PPy-NO_3**: Polypyrrole Nitrate, **$TDANO_3$**: Tridodecylmethylammonium nitrate, **$THANO_3$**: Trioctylmethylammonium nitrate, **$Co(Bphen)_2(NO_3)_2(H_2O)_2$**: Cobalt(II) complex with bathophenanthroline

4. Comparison of selectivity coefficients of nitrate selective electrodes

Table S2: Selectivity comparison for nitrate selective electrodes

References	Interferents	$\mathrm{Log}K_{A,B}^{pot}$
[S4]	Cl^-, HCO_3^-, CH_3COO^-, NO_2^-, SO_4^{2-}	-1.14, -1.47, -1.52, -1.09, -2.04
[S5]	Cl^-, NO_2^-, HCO_3^-, SO_4^{2-}	-1.70, -1.61, -2.93, -2.43
[S6]	SO_4^{2-}, Br^-, Cl^-, CO_3^{2-}, I^-, K^+, Na^+, Mg^{2+}	-5.4, -3.8, -3.1, -4.8, -2.8, -5.7, -4.5, -3.6
[S8]	Cl^-, $H_2PO_4^-$, SO_4^{2-}	-2.55, -4.11, -4.07
[S10]	NO_2^-, Cl^-, $H_2PO_4^-$, CH_3COO^-, CO_3^{2-}, SO_4^{2-}	-1.7, -1.85, -2.70, -2.85, -3.19, -3.40
[S11]	Cl^-, Br^-, SO_4^{2-}, PO_4^{3-}	-1.51, -0.85, -3.21, -3.19
[S13]	SO_4^{2-}, F^-, Cl^-, Br^-, NO_2^-, ClO_4^-	-4.8, -4.4, -3.6, -2.9, -1.9, 2.8
[S14]	$H_2PO_4^-$, SO_4^{2-}, CO_3^{2-}, CH_3COO^-, F^-, Cl^-, NO_2^-, Br^-	-6.02, -5.56, -5.20, -4.55, -4.62, -2.87, -2.29, -1.23
[S15]	$H_2PO_4^-$, SO_4^{2-}, CO_3^{2-}, CH_3COO^-, F^-, Cl^-, NO_2^-, Br^-, SCN^-, ClO_4^-	-5.1, -4.8, -4.9, -4.4, -4.6, -2.6, -2.1, -1.0, 2.1, 3.3
[S16]	Cl^-, CO_3^{2-}, SO_3^{2-}	-1.11, -1.41, -2
[S17]	Cl^-	-1.8
[S18]	Cl^-, SO_4^{2-}, S^{2-}, F^-, CH_3COO^-, PO_4^{3-}, NO_2^-	-5.10, -6.50, -4.70, -6.80, -3.30, -7.10, -4.10
[S19]	Cl^-, SO_4^{2-}, HCO_3^-, $H_2PO_4^-$, HPO_4^{2-}	-2.00, -3.04, -2.15, -3.30, -3.22
Our Work	**Cl^-, F^-, HCO_3^-, ClO_3^-, HPO_4^{2-}, $S_2O_3^{2-}$, CO_3^{2-}, SO_4^{2-}**	**-1.65, -3.24, -3.02, -2.53, -3.11, -3.57, -3.55, -3.82**

5. Determination of the lifetime of the cNSE

To determine the lifetime of the cNSE, calibration curves were created by taking measurements on different days in nitrate solutions within the concentration range of 1.0×10^{-5} to 1.0×10^{-1} M. Figure S1 reveals a decline in the slope of the cNSE around the fifteenth day. For commercial electrodes, the lifespan is defined as the time taken for the electrode's slope to decrease to ~70% of its initial value. Accordingly, for the cNSE the initial slope value (-53.1 mV per decade concentration change) should decrease to 37.1 mV per decade concentration change by the end of its usage period. It was observed that after 14 days of use, the slope of the electrode reduced to ~35.6 mV per decade concentration change. As a result, the lifespan of the cNSE could be estimated to be ~14 days. Before measurements were taken, the electrodes were conditioned in a 1.0×10^{-2} M NO_3^- solution for 30 min. When not in use, the electrodes were stored in a closed and dark environment at room conditions.

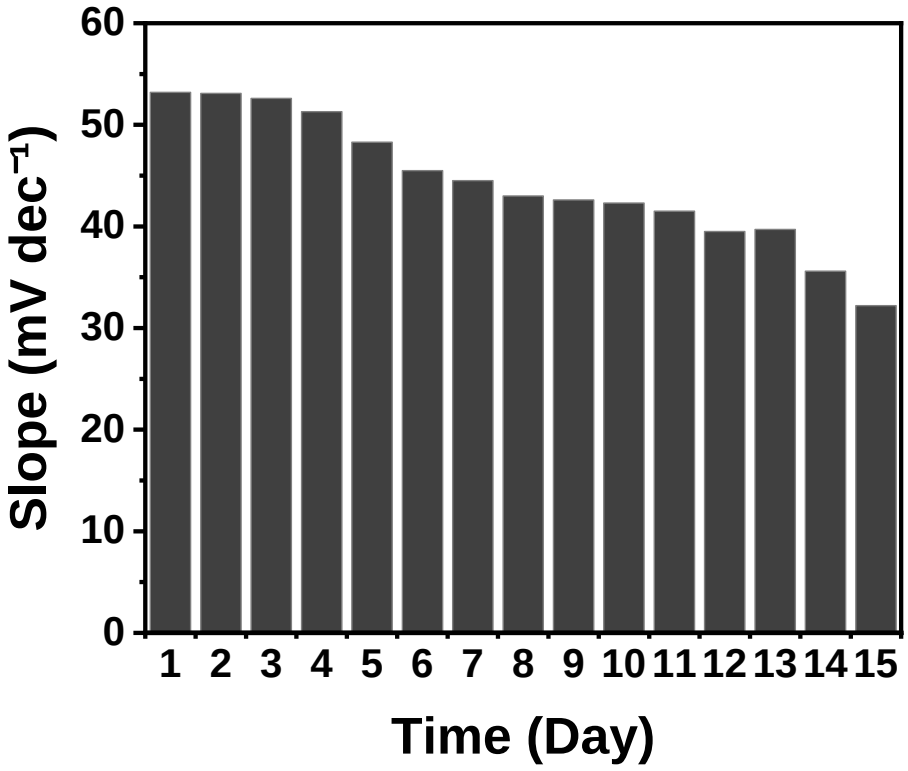

Figure S1: Change in the slope of the cNSE with time (days)

5- Computational calculations of CAGE molecules-nitrate binding

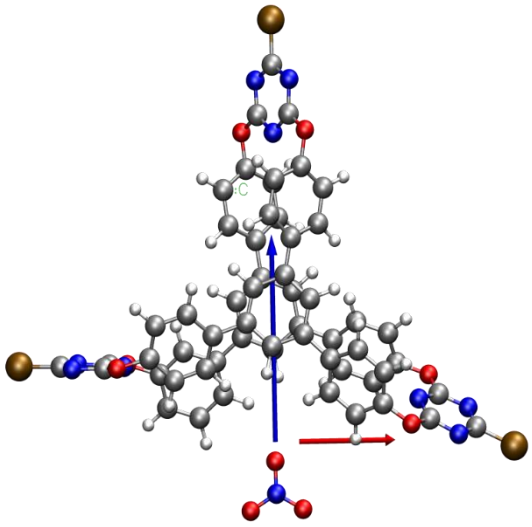

Figure S2: Paths created for PES

The potential energy surface (PES) of CAGE molecules (E2, E4, E5, and E6) interacting with nitrate (NO_3^-) was investigated to identify the most stable conformer using the GNF2-xTB level of theory [S21]. The study began by scanning along a "blue path," where the nitrate molecule was positioned 5 Å from the geometric center of the CAGE molecule, extending toward the triazine group. The nitrate was rotated both on-axis (120°) and off-axis (90°) in 0.5 Å steps to explore various binding geometries. Subsequently, the most stable structures for each CAGE molecule were refined by scanning along a "red path" to further optimize the energy and geometry of the resulting complexes. (Figure S2) Molecules were optimized using DFT with the B3LYP-D3 functional and the def2-TZVP basis set. Frequency calculations were carried out for all optimized geometries at the same level of theory. None of the optimized geometries show any imaginary frequency values. The ground state calculations were performed using the CPCM (conductor-like polarizable continuum model) with water as the solvent. All quantum chemical calculations have been carried out with ORCA 5.0.4 code [S22-S23].

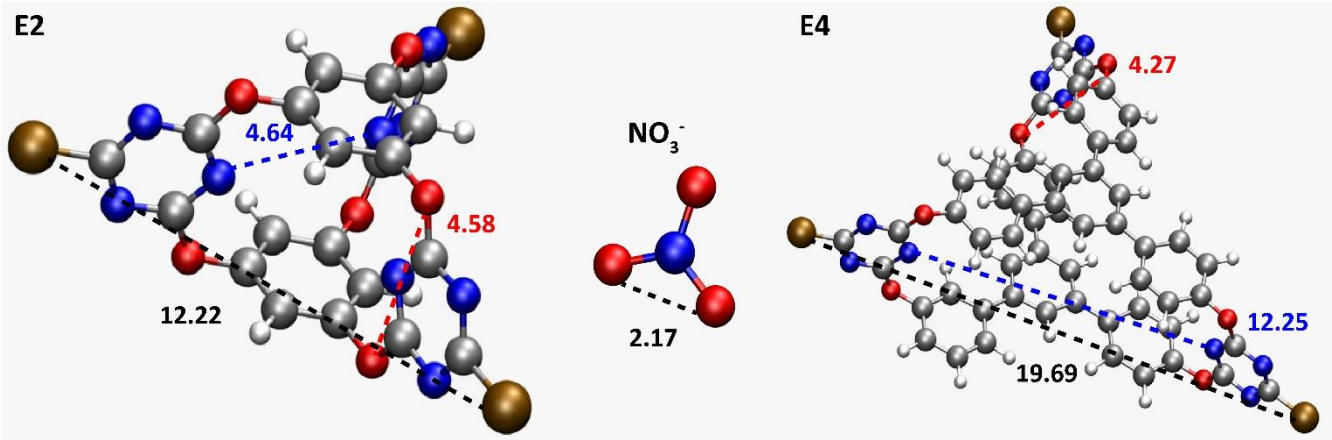

Figure S3: The sizes of the E2 (CAGE-0) and E4 (CAGE-1).

REFERENCES

[S1] Kotha, S., Kashinath, D., & Kumar, S. (2008). Synthesis of liquid crystalline materials based on 1, 3, 5-triphenylbenzene and 2, 4, 6-triphenyl-1, 3, 5-s-triazine. Tetrahedron Letters, 49(37), 5419-5423.

[S2] Wang, D. X., Wang, Q. Q., Han, Y., Wang, Y., Huang, Z. T., & Wang, M. X. (2010). Versatile anion–π interactions between halides and a conformationally rigid bis (tetraoxacalix [2] arene [2] triazine) cage and their directing effect on molecular assembly. Chemistry–A European Journal, 16(44), 13053-13057.

[S3] Naseer, M. M., Wang, D. X., Zhao, L., Huang, Z. T., & Wang, M. X. (2011). Synthesis and functionalization of heteroatom-bridged bicyclocalixaromatics, large molecular triangular prisms with electron-rich and-deficient aromatic interiors. The Journal of Organic Chemistry, 76(6), 1804-1813.

[S4] Paré, F.; Visús, A.; Gabriel, G.; Baeza, M. Novel Nitrate Ion-Selective Microsensor Fabricated by Means of Direct Ink Writing. Chemosensors 2023, 11, 174.

[S5] Hjort, R.G.; Soares, R.R.A.; Li, J.; Jing, D.; Hartfiel, L.; Chen, B.; Van Belle, B.; Soupir, M.; Smith, E.; McLamore, E.; et al. Hydrophobic Laser-Induced Graphene Potentiometric Ion-Selective Electrodes for Nitrate Sensing. Microchim. Acta 2022, 189, 122.

[S6] Thuy, N.T.D.; Wang, X.; Zhao, G.; Liang, T.; Zou, Z. A Co3O4 Nanoparticle-Modified Screen-Printed Electrode Sensor for the Detection of Nitrate Ions in Aquaponic Systems. Sensors 2022, 22, 9730.

[S7] Pietrzak, K.;Wardak, C.; Malinowski, S. Application of Polyaniline Nanofibers for the Construction of Nitrate All-Solid-State Ion-Selective Electrodes. Appl. Nanosci. 2021, 11, 2823–2835.

[S8] Zhang, Z.; Papautsky, I. Miniature Ion-selective Electrodes with Mesoporous Carbon Black as Solid Contact. Electroanalysis 2021, 33, 2143–2151.

[S9] Ali, A.;Wang, X.; Chen, Y.; Jiao, Y.; Mahal, N.K.; Moru, S.; Castellano, M.J.; Schnable, J.C.; Schnable, P.S.; Dong, L. Continuous Monitoring of Soil Nitrate Using a Miniature Sensor with Poly(3-Octyl-Thiophene) and Molybdenum Disulfide Nanocomposite. ACS Appl. Mater. Interfaces 2019, 11, 29195–29206.

[S10] Fozia; Zhao, G.; Nie, Y.; Jiang, J.; Chen, Q.;Wang, C.; Xu, X.; Ying, M.; Hu, Z.; Xu, H. Preparation of Nitrate Bilayer Membrane Ion-Selective Electrode Modified by Pericarpium Granati-Derived Biochar and Its Application in Practical Samples. Electrocatalysis 2023, 14, 534–545.

[S11] Zhang, L.; Wei, Z.; Liu, P. An All-Solid-State NO3 Ion-Selective Electrode with Gold Nanoparticles Solid Contact Layer and Molecularly Imprinted Polymer Membrane. PLoS ONE 2020, 15, e0240173

[S12] Baumbauer, C.L.; Goodrich, P.J.; Payne, M.E.; Anthony, T.; Beckstoffer, C.; Toor, A.; Silver, W.; Arias, A.C. Printed Potentiometric Nitrate Sensors for Use in Soil. Sensors 2022, 22, 4095.

[S13] Liu, Y.; Liu, Y.; Meng, Z.; Qin, Y.; Jiang, D.; Xi, K.;Wang, P. Thiol-Functionalized Reduced Graphene Oxide as Self-Assembled Ion-to-Electron Transducer for Durable Solid-Contact Ion-Selective Electrodes. Talanta 2020, 208, 120374.

[S14] Pietrzak, K.; Wardak, C. Comparative Study of Nitrate All Solid State Ion-Selective Electrode Based on Multiwalled Carbon Nanotubes-Ionic Liquid Nanocomposite. Sens. Actuators B Chem. 2021, 348, 130720.

[S15] Pietrzak, K.; Wardak, C.; Łyszczek, R. Solid Contact Nitrate Ion-selective Electrode Based on Cobalt(II) Complex with 4,7- Diphenyl-1,10-phenanthroline. Electroanalysis 2020, 32, 724–731.

[S16] Kim, M.-Y.; Lee, J.-W.; Park, D.J.; Lee, J.-Y.; Myung, N.V.; Kwon, S.H.; Lee, K.H. Highly Stable Potentiometric Sensor with Reduced Graphene Oxide Aerogel as a Solid Contact for Detection of Nitrate and Calcium Ions. J. Electroanal. Chem. 2021, 897, 115553.

[S17] Ivanova, A.; Mikhelson, K. Electrochemical Properties of Nitrate-Selective Electrodes: The Dependence of Resistance on the Solution Concentration. Sensors 2018, 18, 2062.

[S18] Hassan, S.S.M.; Eldin, A.G.; Amr, A.E.-G.E.; Al-Omar, M.A.; Kamel, A.H.; Khalifa, N.M. Improved Solid-Contact Nitrate Ion Selective Electrodes Based on Multi-Walled Carbon Nanotubes (MWCNTs) as an Ion-to-Electron Transducer. Sensors 2019, 19, 3891.

[S19] Fukao, Y.; Kitazumi, Y.; Kano, K.; Shirai, O. Construction of Nitrate-Selective Electrodes and Monitoring of Nitrates in Hydroponic Solutions. Anal. Sci. 2018, 34, 1373–1377.

[S20] Pi ̨ek, M.; Piech, R.; Paczosa-Bator, B. TTF-TCNQ Solid Contact Layer in All-Solid-State Ion-Selective Electrodes for Potassium or Nitrate Determination. J. Electrochem. Soc. 2018, 165, B60–B65.

[S21] C. Bannwarth, S. Ehlert, S. Grimme, GFN2-xTB - An Accurate and Broadly Parametrized Self-Consistent Tight-Binding Quantum Chemical Method with Multipole Electrostatics and Density-Dependent Dispersion Contributions, J Chem Theory Comput 15 (2019) 1652–1671. https://doi.org/10.1021/acs.jctc.8b01176.

[S22] F. Neese, Software update: The ORCA program system—Version 5.0, Wiley Interdiscip Rev Comput Mol Sci 12 (2022). https://doi.org/10.1002/wcms.1606.

[S23] F. Neese, The ORCA program system, WIREs Computational Molecular Science 2 (2012) 73–78. https://doi.org/10.1002/wcms.81.